The Plant Cell, Vol. 13, 2761–2775, December 2001, www.plantcell.org © 2001 American Society of Plant Biologists

A Novel Family of Magnesium Transport Genes in Arabidopsis

Legong Li,[a,1] Ana F. Tutone,[b,1] Revel S. M. Drummond,[b] Richard C. Gardner,[b,2] and Sheng Luan[a,2]

[a] Department of Plant and Microbial Biology, University of California, Berkeley, California 94720
[b] School of Biological Sciences, University of Auckland, Auckland, New Zealand

Magnesium (Mg^{2+}) is the most abundant divalent cation in plant cells and plays a critical role in many physiological processes. We describe the identification of a 10-member Arabidopsis gene family (*AtMGT*) encoding putative Mg^{2+} transport proteins. Most members of the *AtMGT* family are expressed in a range of Arabidopsis tissues. One member of this family, *AtMGT1*, functionally complemented a bacterial mutant lacking Mg^{2+} transport capability. A second member, *AtMGT10*, complemented a yeast mutant defective in Mg^{2+} uptake and increased the cellular Mg^{2+} content of starved cells threefold during a 60-min uptake period. ^{63}Ni tracer studies in bacteria showed that *AtMGT1* has highest affinity for Mg^{2+} but may also be capable of transporting several other divalent cations, including Ni^{2+}, Co^{2+}, Fe^{2+}, Mn^{2+}, and Cu^{2+}. However, the concentrations required for transport of these other cations are beyond normal physiological ranges. Both *AtMGT1* and *AtMGT10* are highly sensitive to Al^{3+} inhibition, providing potential molecular targets for Al^{3+} toxicity in plants. Using green fluorescence protein as a reporter, we localized AtMGT1 protein to the plasma membrane in Arabidopsis plants. We suggest that the *AtMGT* gene family encodes a Mg^{2+} transport system in higher plants.

INTRODUCTION

Magnesium (Mg^{2+}) is the most abundant divalent cation in a living cell and serves as a cofactor with ATP in a number of enzymatic reactions. In addition, free Mg^{2+} stabilizes membranes and regulates many cellular enzymes. In higher plants, Mg^{2+} plays an even more prominent role because it is an essential component of chlorophyll molecules. Despite these critical cellular functions, Mg^{2+} uptake, transport, and homeostasis in eukaryotes are poorly understood at both the physiological and the molecular level.

Mg^{2+} is unique among the major biological cations in its chemical properties. It has the largest hydrated radius, the smallest ionic radius, and the highest charge density. Because it binds water molecules three to four orders of magnitude more tightly than do other cations, Mg^{2+} often interacts with other molecules while maintaining its hydration sphere. As a result, it is speculated that Mg^{2+} transport systems may use unique membrane channels or carriers (Gibson et al., 1991). Studies of Mg^{2+} transport in bacteria support this hypothesis. The major Mg^{2+} transport genes in bacteria belong to the CorA family, originally identified from *Salmonella typhimurium* (reviewed by Smith and Maguire, 1998). CorA is a single gene locus in *S. typhimurium* encoding a 37-kD integral membrane protein (Smith et al., 1993). Topological analyses of CorA protein reveal a unique structure that contains a large, acidic, N-terminal, periplasmic domain and three transmembrane (TM) domains at the C-terminal region (Smith et al., 1993).

MgtA and MgtB are additional Mg^{2+} transport genes found in *S. typhimurium.* Both are large multi-TM proteins that belong to the P-type ATPases (Maguire, 1992). Both the CorA and Mgt*A*/*B* systems are capable of transporting other divalent cations such as Ni^{2+} and Co^{2+} (Smith and Maguire, 1998; Moncrief and Maguire, 1999). However, the physiologically relevant function of all these genes is their action as Mg^{2+} uptake systems, based on their relative K_m values for these cations and the concentrations of the cations usually encountered by bacteria (Smith and Maguire, 1998).

A recent study has identified two yeast proteins referred to as ALR1 and ALR2 for their function in aluminum resistance (MacDiarmid and Gardner, 1998). These proteins show some similarity to CorA and are required for yeast growth under low concentrations of Mg^{2+}, suggesting that ALR proteins may serve as Mg^{2+} transporters (MacDiarmid and Gardner, 1998). Recently, another yeast protein, MRS2, which also has structural similarity to the bacterial CorA family, has been suggested as a transporter of Mg^{2+} across the inner mitochondrial membrane (Bui et al., 1999). Overexpression of bacterial CorA in the mitochondrial membrane compensated for the loss of Mg^{2+} content in mitochondria

[1] These authors contributed equally to this research.
[2] To whom correspondence should be addressed. E-mail r.gardner@auckland.ac.nz or sluan@nature.berkeley.edu; fax 649-373-7416 (Gardner) or 510-642-4995 (Luan).
Article, publication date, and citation information can be found at www.plantcell.org/cgi/doi/10.1105/tpc.010352.

in an *mrs2* deletion strain. The yeast MRS2, ALR1, and ALR2 proteins share some structural features with the bacterial Mg^{2+} transporter CorA. All have a highly charged N-terminal domain and two hydrophobic regions near the C terminus (MacDiarmid and Gardner, 1998; Bui et al., 1999). There is also an absolutely conserved GMN motif near the end of one of the hydrophobic regions, and mutagenesis of CorA has shown that these three conserved residues are essential for functional Mg^{2+} transport (Szegedy and Maguire, 1999). There may be differences in the number of TM domains in various members of the family, because MRS2 protein has been shown to possess only two TM domains (Bui et al., 1999), in contrast to the three found in CorA (Smith et al., 1993).

To date, the only Mg^{2+} transport protein characterized from a multicellular organism is the Mg^{2+}/H^+ exchanger in Arabidopsis, AtMHX (Shaul et al., 1999). Very similar to animal Ca^{2+}/Na^+ exchangers, AtMHX is localized to the tonoplast and mediates transport of Mg^{2+} into the vacuole in a proton-dependent manner (Shaul et al., 1999). Here, we report identification of a family of Mg^{2+} transporters from Arabidopsis that are homologous to the yeast *MRS2* gene and to the CorA family in bacteria. The family has 10 members, most of which are expressed in a range of plant tissues. One family member, *AtMGT1*, functionally complements an Mg^{2+} transport mutant of *S. typhimurium*, whereas a second member, *AtMGT10*, complements an equivalent yeast mutant. AtMGT1-mediated uptake of cations into bacteria showed similar kinetics to that of CorA, a high-affinity Mg^{2+} transporter in bacteria. We also present evidence that suggests a plasma membrane localization of AtMGT1 in Arabidopsis, which is consistent with a possible function of AtMGT1 in Mg^{2+} uptake and translocation.

RESULTS

AtMGT10 Complements a Yeast Strain Deficient in Mg^{2+} Uptake

The first member of the Arabidopsis gene family was identified by complementation of a yeast mutant (CM66) that lacks both the *ALR1* and *ALR2* genes, and therefore cannot grow on standard synthetic media (SD) containing 4 mM Mg^{2+} (Sherman, 1991). This strain was used to screen the Lacroute cDNA library (Minet et al., 1992) for Arabidopsis genes that confer the ability to grow on 4 mM Mg^{2+}. From ~1.5 million transformants, we obtained a single plant cDNA that appeared to be altering Mg^{2+} uptake. This plasmid was completely sequenced. It contained a gene that has been called *AtMGT10* (for *Arabidopsis thaliana* magnesium transport; numbering is derived from analysis of the family [see below]). Figure 1A shows that expression of this plant gene is able to complement growth on solid medium with 4 mM Mg^{2+}. However, the plant gene is not as effective as is the endogenous yeast *ALR1* gene in allowing growth at lower levels of Mg^{2+} (Figure 1B).

AtMGT10 is able to direct Mg^{2+} uptake into yeast over a short time frame. Yeast strains were grown at high Mg^{2+} (250 mM) and then starved by growing them for 24 hr in minimal media lacking Mg^{2+}. Figure 2A shows that before starvation, the steady state Mg^{2+} content of the mutant strain CM66 expressing *AtMGT10* was 34% higher than that

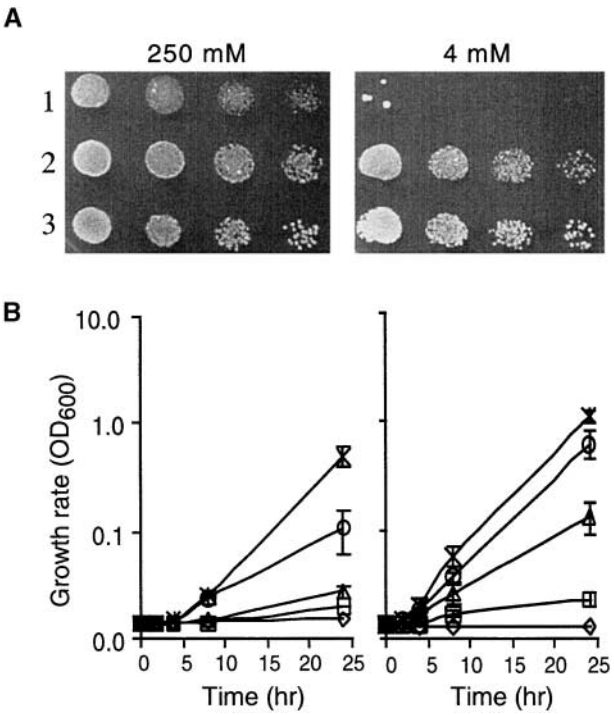

Figure 1. *AtMGT10* Allows Growth of Mg^{2+}-Deficient Yeast.

(A) Complementation on solid medium. CM66 and CM52 cells containing various plasmids were grown to saturation in SDM-ura medium (see Methods), washed free of excess Mg^{2+} with water, and diluted to give similar OD_{600} readings; fivefold dilutions were applied to SD-ura plates containing 4 mM or 250 mM Mg^{2+}. Row 1, CM66 + pFLN2; row 2, CM66 + pFL61-*AtMGT10*; row 3, CM52 + pFLN2-*ALR1*. Plates were photographed after 3 days at 30°C.

(B) Growth in liquid medium. CM66 cells overexpressing either *AtMGT10* (left) or the yeast *ALR1* gene (right) were grown in SDM-ura to log phase (OD_{600} = 0.6 to 0.8). The cells were harvested by centrifugation, washed twice with distilled water to remove traces of Mg^{2+}, and resuspended in distilled water. Aliquots of 25 mL of LPM (see Methods) were prepared containing increasing concentrations of $MgCl_2$; 0 μM (open diamond), 5 μM (open square), 20 μM (open triangle), 100 μM (open circle), and 4000 μM (x). CM66 cells were then added to give a final A_{600} of 0.001 to 0.002. The growth of the cultures was monitored over 24 hr by following OD_{600}. Results displayed are averages (±SE) for three cultures grown on different days.

of the same strain containing the vector. However, during the 24 hr of starvation, Mg^{2+} content decreased to similar levels in both strains (Figure 2A). Mg^{2+} uptake into the starved cells was then compared at 4 mM Mg^{2+} over a 60-min period. In CM66 expressing AtMGT10, the total intracellular Mg^{2+} content doubled after 20 min and increased more than threefold after an hour. In contrast, intracellular Mg^{2+} content in the control strain increased by only 41% in an hour (Figure 2B).

AtMGT Is Encoded by a Multigene Family in Arabidopsis

We have identified from the Arabidopsis genome database a family of 10 genes encoding proteins related to AtMGT10. We refer to the genes as *AtMGT1* to *AtMGT10*. cDNA copies of *AtMGT1* to *AtMGT9* were amplified by reverse transcription–polymerase chain reaction (RT-PCR) and sequenced to confirm the protein sequence; in five cases, the actual sequence differed from splice site predictions in the database (see Methods).

An amino acid comparison of the Arabidopsis proteins and their homologs is shown in Figure 3A. The gene family is most similar to two yeast proteins, including MRS2, which is involved with Mg^{2+} uptake into mitochondria (Bui et al., 1999). In addition, we recently isolated homologous cDNAs from human and rat. The human protein has a mitochondrial leader and can complement mitochondrial Mg^{2+} transport in *mrs2* yeast (Zsurka et al., 2001). The 10 Arabidopsis family members showed significant amino acid diversity, with amino acid identities ranging from 15 to 89%. However, there are six motifs conserved across the whole family (shown in boldface in Figure 3A); none of these appears to correspond to known functional groups identified to date. The conserved GMN motif near the C terminus is also present in the bacterial and yeast members of the CorA family, where it is located in one of the two TM domains. Even conservative changes in these residues inactivate CorA (Szegedy and Maguire, 1999).

The phylogenetic relationship between the amino acid sequences of the yeast, mammalian, and Arabidopsis genes is shown in Figure 3B. The yeast and mammalian genes group separately on the tree from the plant genes, as expected. Several of the Arabidopsis genes grouped in clusters on the tree. For example, *AtMGT1* and *AtMGT2*, *AtMGT5* and *AtMGT6*, and *AtMGT7*, *AtMGT8*, and *AtMGT9* appear to be closely related. *AtMGT10* is the most divergent of the plant family.

Figure 3C shows the approximate locations of introns in the 10 Arabidopsis genes. The number and location of splice sites vary widely between some genes (e.g., *AtMGT10* and all the others), with some others identical (e.g., *AtMGT7* to *AtMGT9*). The relationship between the number and location of splice sites in each gene (Figure 3C) closely reflects the phylogenetic relationships between the amino acid sequences shown in Figure 3B. The genes map to all five chromosomes and, except for *AtMGT7* and *AtMGT8*, are located on different bacterial artificial chromosomes. On the basis of a comparison of their locations and the chromosomal relationships (Blanc et al., 2000), researchers have found no obvious indication that any of the genes have arisen by polyploidization of the Arabidopsis genome.

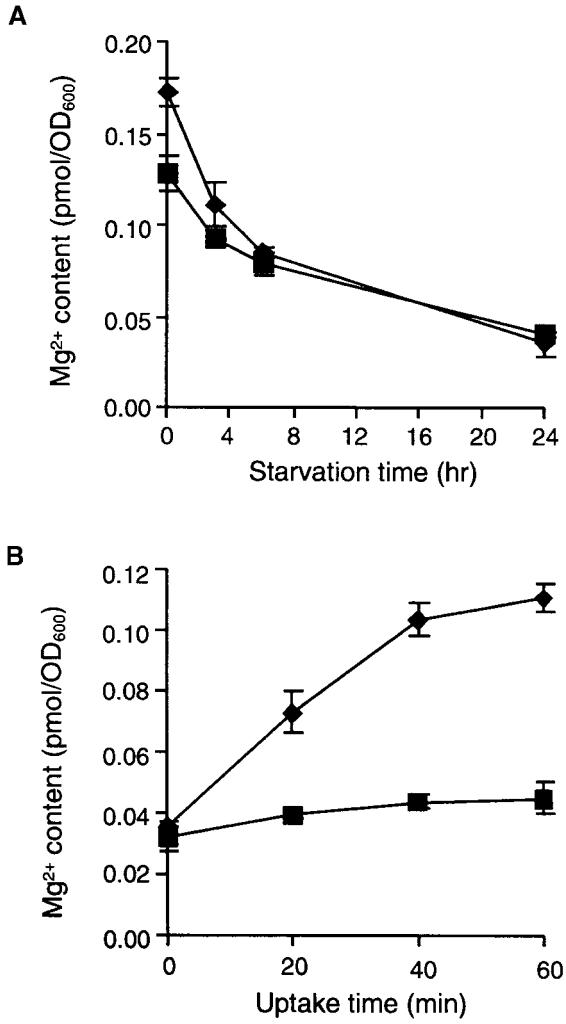

Figure 2. Uptake of Mg^{2+} in Yeast by AtMGT10.

(A) Time course of Mg^{2+} starvation. The Mg^{2+} content is shown for yeast cells pre-grown in minimal (SD) medium containing 250 mM Mg^{2+} and then cultured for 24 hr in media without Mg^{2+}. Diamonds, pFL61-AtMGT10/CM66; squares, pFLN2/CM66. Results are averages (±SE) of duplicate measurements made for three cultures grown on different days.

(B) AtMGT10 mediates Mg^{2+} uptake. Starved cells were pre-incubated with glucose, and then Mg^{2+} uptake was measured in succinate buffer, pH 4, with 4 mM Mg for 1 hr. Symbols and measurements are as given in **(A)**.

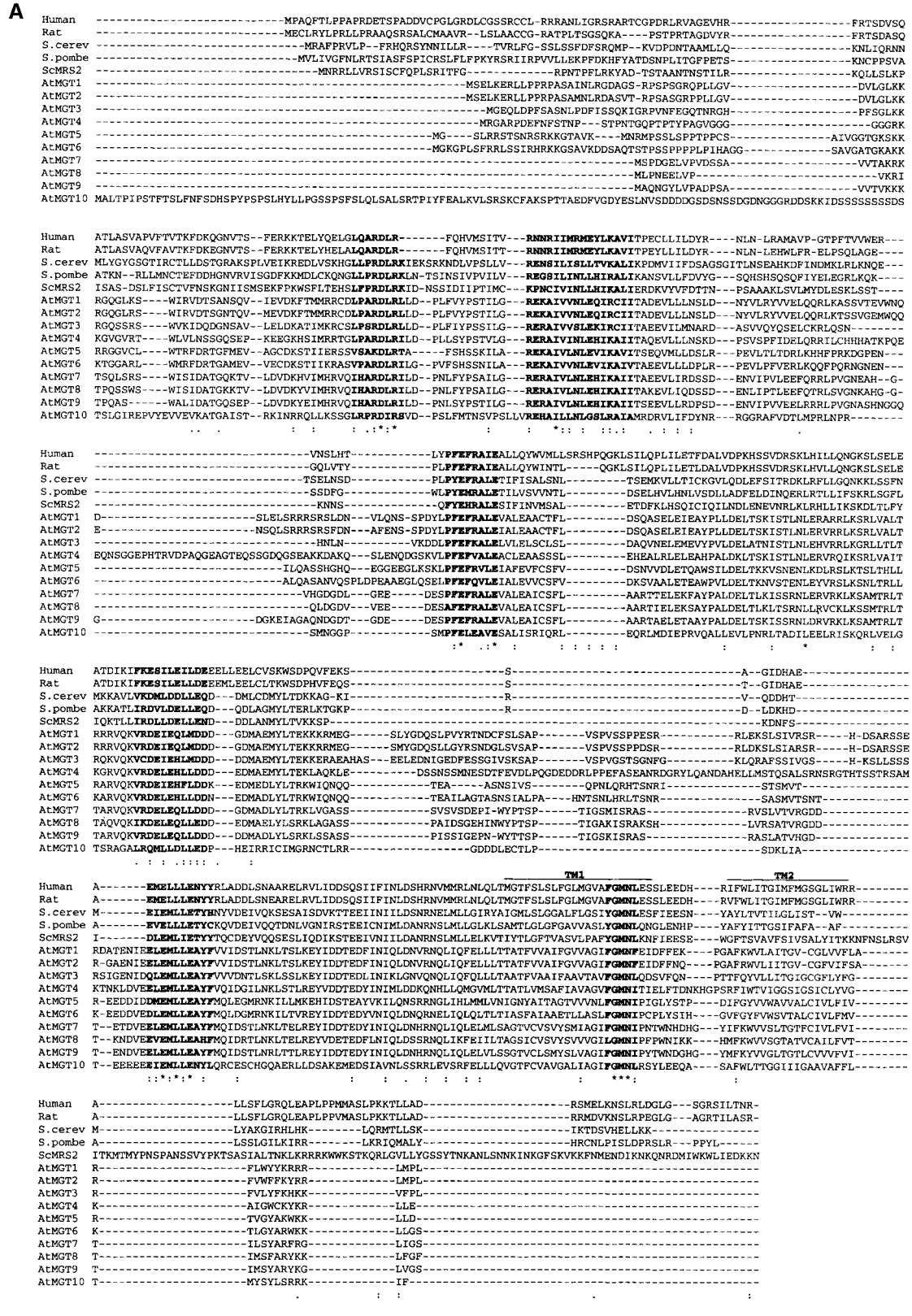

Figure 3. Analysis of the AtMGT Family.

MGT Family Is Expressed in Most Tissues of Arabidopsis

RT-PCR was used to detect expression of all 10 members of the gene family from a range of different tissues; the results are shown in Figure 4. Products of the expected size were amplified from almost all samples by using primers corresponding to *AtMGT1* to *AtMGT10*. There was little evidence for specificity of gene expression between different tissues, with the exception of *AtMGT5*, whose transcript was detected only in floral tissues. *AtMGT8* transcript was not detected in stems.

AtMGT1 Functionally Complements a Salmonella Mutant Lacking CorA, MgtA, and MgtB

To further determine whether AtMGT proteins serve as Mg^{2+} transporters, we examined the function of the AtMGT1 protein in bacteria. The AtMGT1 protein was expressed in a Salmonella mutant strain lacking Mg^{2+} transporting systems CorA, MgtA, and MgtB. This mutant strain, referred to as MM281, does not grow on media containing low concentrations of Mg^{2+} (<10 mM). In contrast, MM281 transformed with a λYES vector expressing AtMGT1 or Salmonella CorA grew well on media containing 10, 100, or 200 μM $MgSO_4$ (Figure 5). The mutant and all the transformants grew normally on the medium containing 10 mM $MgSO_4$. This result clearly suggests that AtMGT1 protein, like Salmonella CorA, is capable of mediating Mg^{2+} uptake in bacteria under low Mg^{2+} concentration.

AtMGT1 Shows Properties Similar to CorA, a High-Affinity Mg^{2+} Transporter

The transport properties of AtMGT1 were analyzed in uptake experiments using $^{63}Ni^{2+}$ as a tracer, based on previously described procedures (Snavely et al., 1991). A number of studies have demonstrated that Mg^{2+} and Ni^{2+} can use the same transport system in the cell. For example, bacterial CorA transports both Mg^{2+} and Ni^{2+}, although the affinity for Mg^{2+} is 10-fold higher (Smith and Maguire, 1998). Figures 6A and 6B show that the uptake kinetics for Ni^{2+} and Mg^{2+} displayed the same pattern for Salmonella CorA and

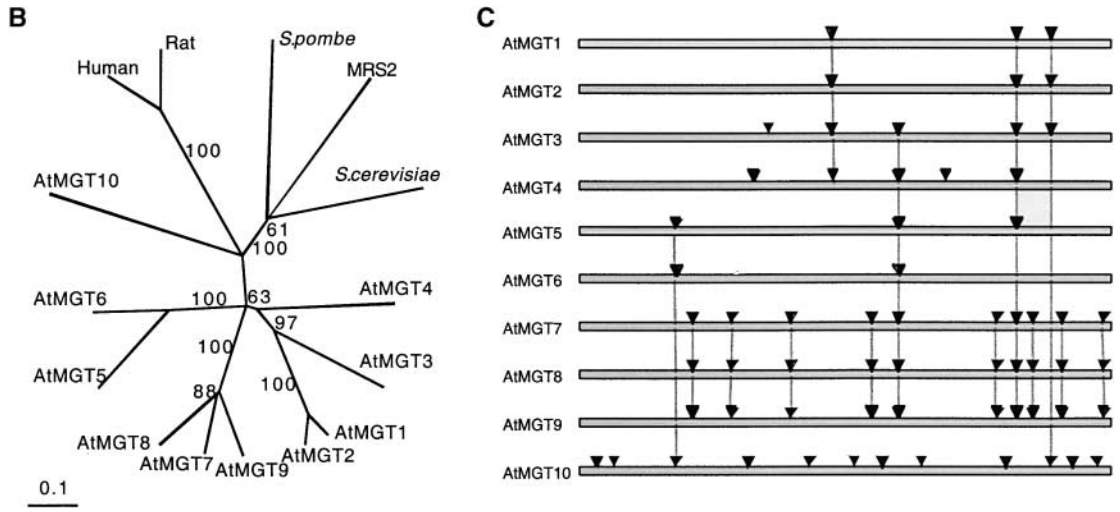

Figure 3. (continued).

(A) ClustalX alignment for the 10 Arabidopsis *MGT* genes and homologs in yeast and mammals. Conserved motifs are indicated in boldface. The protein sequences for *AtMGT1* to *AtMGT9* were derived by translating the genomic sequences, using the splice sites derived from cDNA sequences (see Methods). The accession numbers for the other sequences are as follows: ScMRS2, AAA34795; *Saccharomyces cerevisiae*, "*S. cerevisiae* probable membrane protein" S60930; *S. pombe*, "*S. pombe* unknown protein" T40003; human, AF288288; rat, AF288289; and *AtMGT10*, AF322255.

(B) Unrooted, parsimony-based phylogram of the *MGT* gene family, based on the amino acid sequence alignment shown in **(A)**. The tree was generated using PAUP* 4.0 b5 (D. Swofford, Smithsonian Institution). Bootstrap values >50 are indicated (1000 replicates, full heuristic search option, TBR branch-swapping with random addition). The value of 61 refers to a short branch separating *S. pombe* from the pairing of MRS2 with the other *S. cerevisiae* sequence, whereas the value of 88 refers to the branch separating AtMGT9 from the pairing of AtMGT7 and AtMGT8.

(C) Schematic alignment of the *AtMGT* family with the approximate location of the intron splice sites (solid arrows) indicated. Vertical lines indicate sites whose location is conserved between family members.

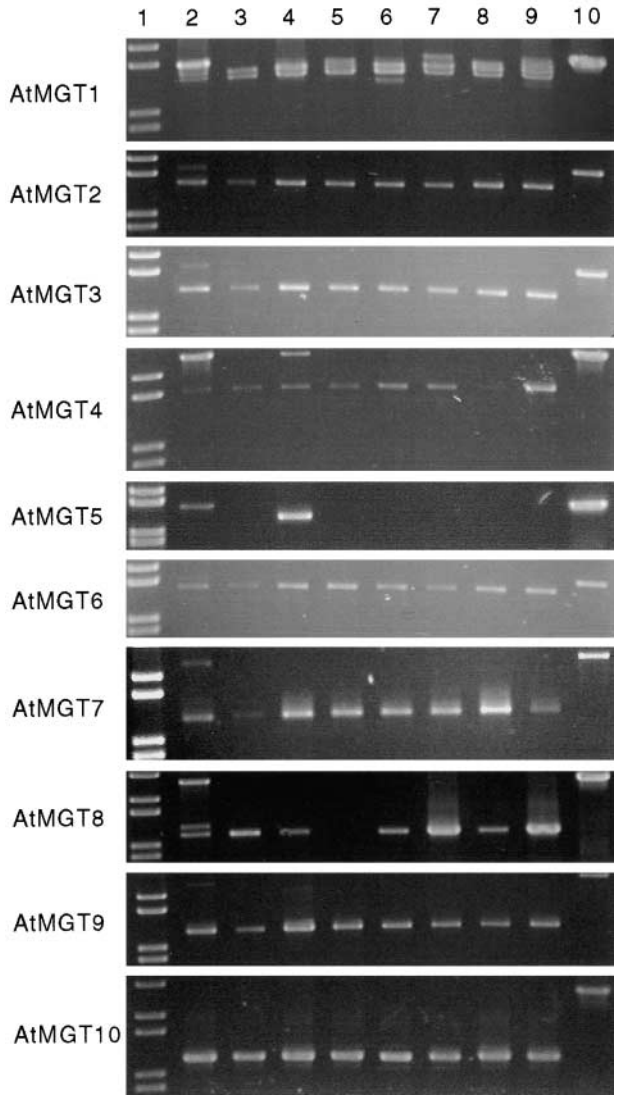

Figure 4. Expression Pattern of the AtMGT Gene Family in Arabidopsis.

RT-PCR products were amplified from mRNA from a variety of plant tissues by using oligonucleotides specific for each of the 10 Arabidopsis AtMGT family members and electrophoresed in 1% TBE (90 mM Tris base, 90 mM Boric acid, 1 mM EDTA, pH 8.0) agarose gels. Lane 1, 1-kb Plus MW markers (Gibco BRL); lanes 2 to 9, RNA isolated from young siliques (2), mature siliques (3), flowers (4), stems (5), leaves (6), roots (7), hydroponically grown leaves (8) and hydroponically grown roots (9); lane 10, amplified products from Arabidopsis genomic DNA. The oligonucleotides used all amplify products in the range of 1.2 to 1.5 kb. Products equal in size to those amplified from genomic DNA are present in all amplifications of mRNA from young siliques (lane 2), as well as in amplifications of mRNA from flower (lane 4) and root (lane 7), using *AtMGT4* and *AtMGT1* primers, respectively.

AtMGT1. In the mutant strain, Ni^{2+} and Mg^{2+} began to inhibit tracer uptake at a concentration of 10 mM, which is consistent with the fact that MM281 required 10 mM $MgSO_4$ to grow. In MM281 expressing either Salmonella CorA or AtMGT1, tracer uptake inhibition took place at Ni^{2+} concentrations of 10 to 100 μM but at 10-fold lower Mg^{2+} concentrations (1 to 10 μM). The Ni^{2+} concentrations required for 50% inhibition of tracer uptake (Ki) were 167 and 128 μM for AtMGT1 and CorA, respectively. The equivalent values for Mg^{2+} were 17 and 15 μM, respectively (Figure 6B). Because AtMGT1 and CorA are comparable in their affinity for Ni^{2+} and Mg^{2+}, the K_m value for Mg^{2+} uptake by AtMGT1 should be in approximately the same range as that of Salmonella CorA (20 to 30 μM; Snavely et al., 1989). This indicates that AtMGT1 may function like CorA, a high-affinity Mg^{2+} transporter.

To further confirm that the transport properties of AtMGT1 are similar to CorA, we tested whether AtMGT1 function is inhibited by cation hexaamines, potent and specific inhibitors for CorA transport activity (Kucharski et al., 2000). Cation hexaamines are chemically stable analogs of the hydrated form of cations, particularly Mg^{2+}. Cobalt(III)-hexaamines are potent inhibitors for CorA, whereas cobalt(III)-chloropentaamines are less potent (Kucharski et al., 2000). When these two compounds were applied to the tracer uptake assays using MM281 strain transformed by *AtMGT1*-containing plasmid, we observed strong inhibition of Ni^{2+} uptake by Co(III)-hexaamine. Co(III)-chloropentaamine also inhibited uptake by AtMGT1 protein but with less potency. As shown in Figure 6C, 0.1 μM Co(III)-hexaamine began to inhibit tracer uptake. The concentration for 50% inhibition was 4.8 μM for Co(III)-hexaamine and 310 μM for Co(III)-chloropentaamine. This result closely matched those from studies on Salmonella CorA inhibition by these compounds (Kucharski et al., 2000).

AtMGT1 Is Highly Selective for Mg^{2+} among Divalent Cations

AtMGT1 functionally complemented a Salmonella mutant lacking Mg^{2+} uptake capability and effectively bound to Mg^{2+} as indicated by the tracer inhibition assays. To further address the functional identity of AtMGT1, we performed tracer inhibition assays with a number of other divalent cations to determine the ionic selectivity of AtMGT1. As shown in Figure 7A, several divalent cations, including Fe^{2+}, Cu^{2+}, Mn^{2+}, and Co^{2+}, significantly inhibited tracer uptake by AtMGT1. However, the concentrations required for inhibition were much higher than those found for Mg^{2+}. For example, the concentrations required for 50% inhibition are in the range of 100 μM to 1 mM for Cu^{2+} and Co^{2+}, and >1 mM for Fe^{2+} and Mn^{2+}. Cadmium (Cd^{2+}) also inhibited tracer uptake but at even higher concentrations (1 to 10 mM). Ca^{2+} and Ba^{2+} did not inhibit tracer uptake even at a concentration of 10 mM (data not shown). These results are very simi-

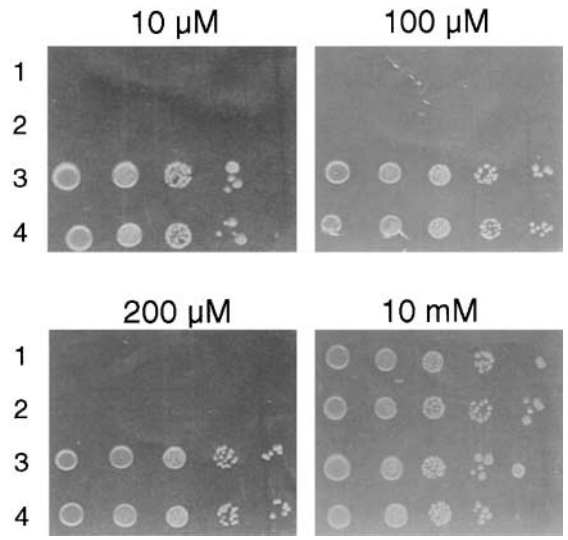

Figure 5. Complementation of the MM281 Mutant by AtMGT1.

Growth of different strains on the N-minimal medium containing 10 μM, 100 μM, 200 μM, and 10 mM $MgSO_4$, respectively. The strains include MM281 (1), MM281 transformed with λYES vector (2), MM1927 (3), and MM281 transformed with AtMGT1 cDNA in λYES vector (4).

lar to those obtained for CorA (Snavely et al., 1989; Smith and Maguire, 1998) and indicate that AtMGT1 is capable of transporting other divalent cations at concentrations beyond physiological range.

Expression of AtMGT1 or AtMGT10 Alters Cation Sensitivity

Excessive accumulation of divalent cations often asserts a toxic effect on microbial cells. To test whether AtMGT1 actually mediates the uptake of those divalent cations, we assayed the cation sensitivity of the mutant and the mutant transformed with the putative transport gene. As shown in Figure 7B, MM281 mutant transformed with AtMGT1 showed significantly higher sensitivity to Fe^{2+} and Cu^{2+} as compared with that of the MM281 mutant. We performed each assay under a series of cation concentrations (0, 10, 100 μM, 1, 10 mM). The difference in cation sensitivity occurred only when the concentration of Fe^{2+} and Cu^{2+} reached 1 mM, suggesting that AtMGT1 may take up these cations at a similar concentration, consistent with the tracer inhibition assays shown in Figure 7A. We also measured sensitivity to Mn^{2+} and Cd^{2+}. Cd^{2+} was toxic to both MM281 and AtMGT1 strains at a low concentration (10 μM), whereas both strains grew well on medium containing 10 mM Mn^{2+} (data not shown).

In addition, we tested the cation sensitivity of the wild-type yeast and the same strain transformed with the AtMGT10 construct. The wild-type yeast was used in the assay because the high levels of Mg^{2+} necessary for growth of the CM66 mutant affect the sensitivity of yeast to other divalent cations (MacDiarmid and Gardner, 1996). Expression of *AtMGT10* altered the sensitivity of yeast to a range of divalent cations. In particular, the strain became more sensitive to Cd^{2+} and Cu^{2+} and more tolerant to Co^{2+} (Figure 7C). We also observed minor increases in sensitivity to Ni^{2+} and in tolerance to Zn^{2+} and Mn^{2+} (data not shown). The strain overexpressing *AtMGT10* also showed tolerance to the trivalent cations La^{3+} and In^{3+} but showed no change in tolerance to Al^{3+} (data not shown).

These results are consistent with the idea that the AtMGT family is capable of transporting other divalent cations in addition to Mg^{2+} and Ni^{2+}. Similar changes in cation sensitivity have been found with other members of the CorA superfamily (Snavely et al., 1989; MacDiarmid and Gardner, 1998; Bui et al., 1999). However, the concentrations of metals used in all these experiments are very high and rarely encountered in natural conditions. We propose that, like other members of the CorA family, AtMGT1 and AtMGT10 are selective Mg^{2+} transporters under normal physiological conditions.

AtMGT1 and AtMGT10, But Not Bacterial CorA, Are Highly Sensitive to Aluminum

In yeast, low concentrations of Al^{3+} have been shown to inhibit uptake of Co^{2+} via the ALR proteins (MacDiarmid and Gardner 1996, 1998). In higher plants, several reports suggest that aluminum ions (Al^{3+}) inhibit cation transport, including Mg^{2+} accumulation (Joslin et al., 1988; Rengel and Robinson, 1989; Tan et al., 1991; Matsumoto, 2000). We speculated that if the AtMGT family plays a role in Mg^{2+} uptake in plants, the AtMGT proteins may be a molecular target for Al inhibition of Mg^{2+} uptake. To test this idea, we included Al^{3+} in the tracer uptake assay for AtMGT1. AtMGT1, but not Salmonella CorA, was sensitive to micromolar levels of aluminum (Figure 8A). Some inhibition of AtMGT1 activity occurred at an Al^{3+}:Ni^{2+} ratio of 1:100 (1 μM Al^{3+} in an assay containing 100 μM Ni^{2+}). At a concentration of 10 μM, Al^{3+} almost completely inhibited the tracer uptake through AtMGT1. The effective concentrations of Al^{3+} are well within the physiological range, because most acidic soils contain micromolar concentrations of Al. Compared with AtMGT1, Salmonella CorA was not inhibited by Al^{3+} unless 1 to 10 mM concentrations were added to the assay (Figure 8A).

AtMGT10-mediated uptake of Mg^{2+} into yeast cells was also very sensitive to Al^{3+} inhibition, as shown in Figure 8B. Inhibition of uptake again occurred at micromolar concentrations, with complete inhibition at 50 μM Al^{3+} (corresponding to an Al^{3+}:Mg^{2+} ratio of 1:80 in the assay conditions).

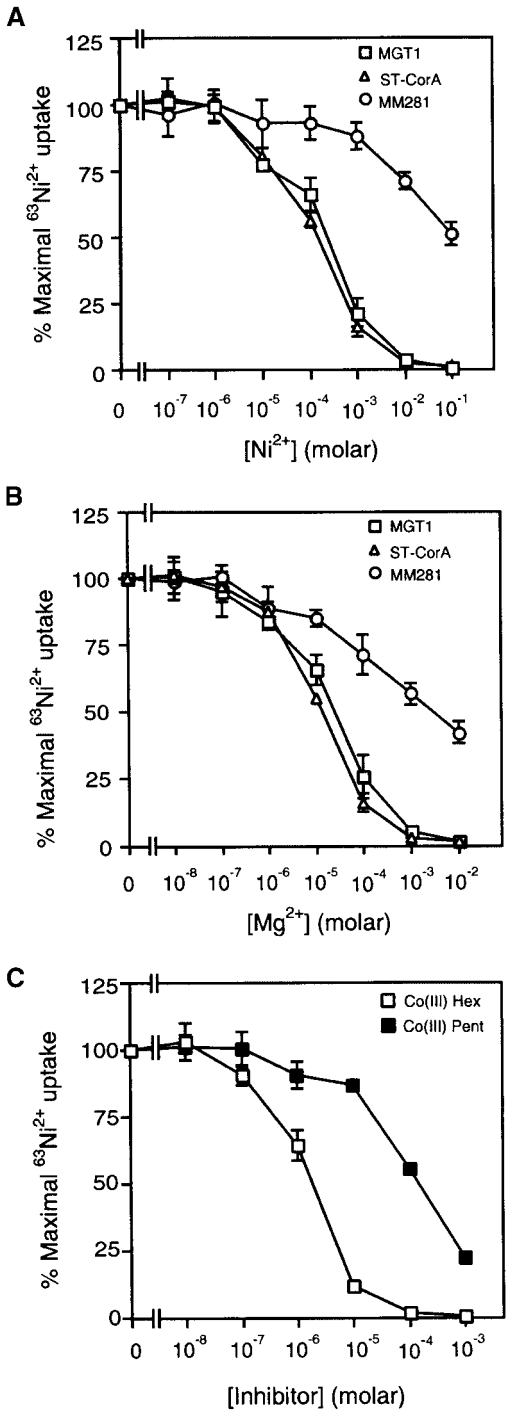

Figure 6. Ni^{2+} and Mg^{2+} Transport Measured by Inhibition of $^{63}Ni^{2+}$ Uptake.

(A) Ni^{2+} inhibition of $^{63}Ni^{2+}$ uptake.
(B) Mg^{2+} inhibition of $^{63}Ni^{2+}$ uptake.
(C) Inhibition of AtMGT1 activity by chloropentaammine and hexaammine.
Transport assay was performed using three Salmonella strains as described in Methods. Tracer uptake is presented as the percentage of the maximal uptake by each strain. Data are average values of three independent experiments and are presented as mean ±SE. Uptake was measured for 5 min with triplicates at each cation concentration. MGT1, MM281 transformed with AtMGT1 cDNA in λYES vector; ST-CorA, MM281 transformed with *S. typhymurium* CorA; MM281, MM281 mutant transformed with λYES vector; Co(III) Pent, Co(III)-chloropentaammines; Co(III) Hex, Co(III)-hexaamine.

AtMGT1-GFP Analysis Suggests Plasma Membrane Localization

As discussed earlier, a Mg/H^+ exchanger has been localized to the tonoplast of Arabidopsis plants, implicating AtMHX in Mg^{2+} accumulation in the vacuole (Shaul et al., 1999). To understand the cellular function of AtMGT family members in plants, it is important to determine the subcellular localization of AtMGT proteins. We began this effort by examining the subcellular location of AtMGT1 protein. We fused AtMGT1 cDNA to a gene coding for green fluorescent protein (GFP) in a binary vector and delivered the construct into Arabidopsis plants. Expression of GFP and AtMGT1-GFP fusion protein was driven by the cauliflower mosaic virus 35S promoter. We determined the subcellular localization of GFP fusion protein by confocal microscopy. In all cell types examined, GFP fluorescence suggested a plasma membrane localization for the fusion protein. Figure 9 presents confocal images of root tip and elongated root cells from the controls and AtMGT1-GFP–expressing plants. We analyzed, for controls, wild-type nontransformed plants, plants transformed with non-fused GFP, and plants expressing a plasma membrane protein fused to GFP. Background signals associated with the root tip region are shown in Figure 9A. Localization of GFP only is shown in Figures 9B and 9G, indicating a ubiquitous localization pattern in plant cells. The defined peripheral localization of a cell surface marker protein fused to GFP is shown in Figure 9C as a positive control for plasma membrane localization. AtMGT1-GFP showed a similar localization pattern, with fluorescence in the periphery of cells of the root tip region and elongation zone (Figures 9D and 9H). In elongated root cells, a large central vacuole occupies most of the cell volume, and plasma membrane and tonoplast are closely located, separated only by a thin layer of cytoplasm. However, cells in the root tip region do not contain large central vacuoles, and the peripheral localization pattern in those cells suggests a plasma membrane association. We also treated the root tips by osmolysis and examined the localization pattern of GFP fluorescence. In plants transformed with the cell surface marker or AtMGT1-GFP fusion, GFP fluorescence was contracted with the cytoplasm after osmolysis (Figures 9E and 9F). This suggests that localization of AtMGT1-GFP fusion with the cell periphery was not the result of cell wall association. Fur-

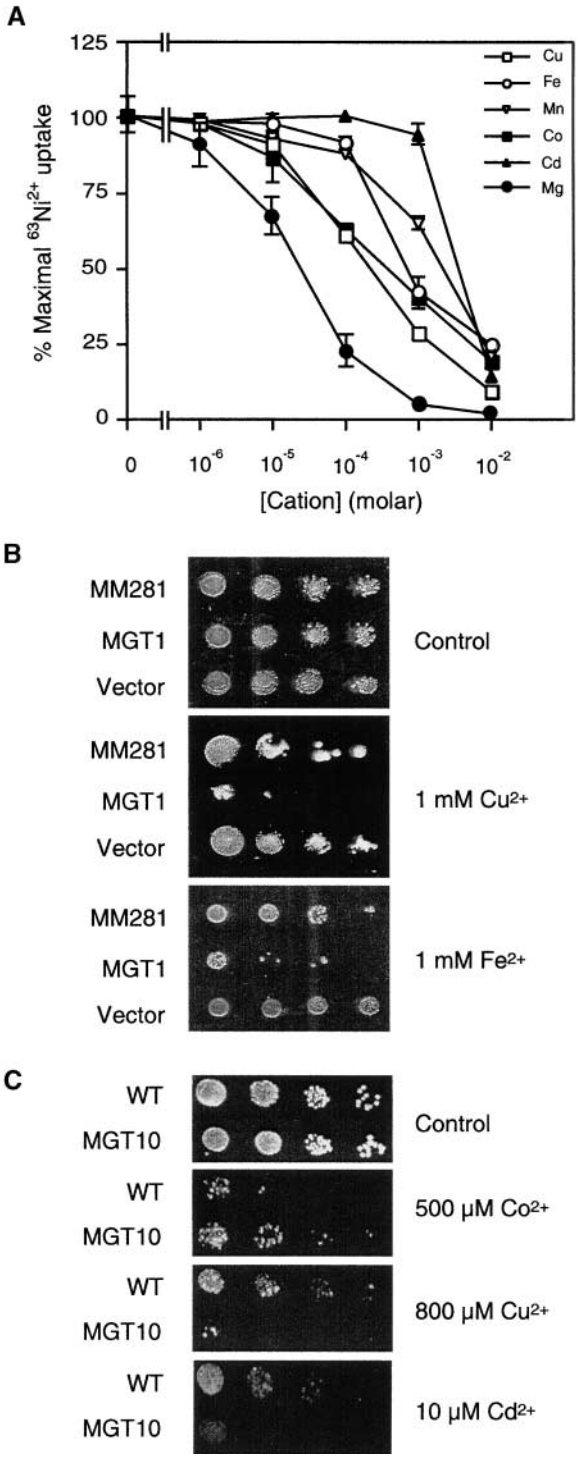

Figure 7. Cation Selectivity of AtMGT1 and AtMGT10.

(A) Inhibition of AtMGT1-mediated tracer uptake by divalent cations. The data shown are normalized to the percentage of control ($^{63}Ni^{2+}$ uptake with 100 μM Ni^{2+} in the solution without other divalent cations). Two independent experiments were performed with Salmonella strains in triplicates at each cation concentration; the data points are shown as mean ±SE.

(B) Cation sensitivity of MM281 mutant (MM281) and mutant strain transformed with AtMGT1 construct (MGT1) or empty vector (Vector).

(C) Cation sensitivity of wild-type yeast strain (WT) and the same strain transformed with AtMGT10 construct (MGT10).

ther confirmation of subcellular localization of AtMGT1 requires precise cellular fractionation and detection of AtMGT1 protein and its activity from each cellular fraction.

DISCUSSION

We have identified a multigene family in Arabidopsis that encodes CorA homologs, and shown that the homologs function as Mg^{2+} transport genes in bacteria and yeast. We suggest that these CorA-like proteins play a role in Mg^{2+} transport in higher eukaryotic organisms. The *AtMGT* family has at least 10 members that most closely resemble the MRS2 gene, which is involved in uptake of Mg^{2+} into yeast mitochondria (Bui et al., 1999). The family bears little similarity to bacterial CorA proteins; most of the identical residues are present in the C-terminal region containing the TM segments in bacterial CorA proteins. The localized homology becomes significant within the putative TM domains. In particular, a GMN amino acid stretch is absolutely conserved in all CorA homologs in bacteria and yeast, as well as in all members of the MRS2 subfamily (Figure 3A). It therefore represents a signature motif of CorA-like Mg^{2+} transporters. The proposed topologies of CorA (Smith et al., 1993) and MRS2 (Bui et al., 1999) differ in one TM domain. However, both topologies place the GMN motif in the same relative location, namely, at the end of a TM domain located very near the outer side of the membrane. This conserved location, combined with the results of CorA mutagenesis studies (Szegedy and Maguire, 1999), suggests that the motif plays a crucial role in the function of the whole CorA family. The proposed TM structure for the MRS2 subfamily of CorA proteins is reminiscent of that determined for the bacterial mechanosensitive cation channel MscL, which has two TM domains and forms homopentamers (reviewed by Rees et al., 2000). The bacterial CorA gene may also function as a homopentamer (Szegedy and Maguire, 1999).

Our studies have demonstrated the function of two members in the AtMGT family by complementation and uptake assays. AtMGT10 suppressed the growth defect in the *alr1alr2* double mutant strain of yeast that does not survive on medium with normal levels of Mg^{2+}. *AtMGT1*, another member of the *AtMGT* family, completely suppressed the

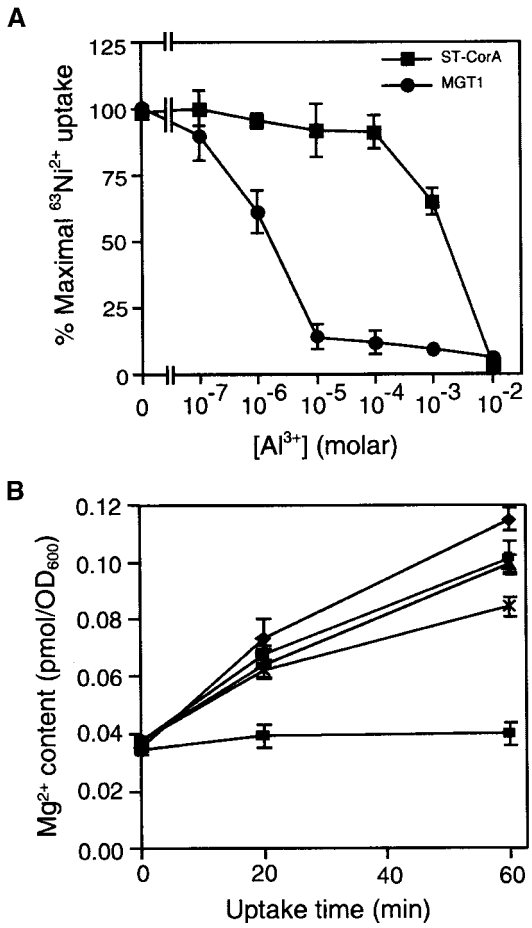

Figure 8. Al^{3+} Inhibition of AtMGT Transport.

(A) Al^{3+} inhibition of AtMGT1 activity. Data shown are normalized as percentage of the maximal uptake in the absence of Al. The data for AtMGT1-transformed MM281 strain are the averages of three independent experiments, whereas those for CorA-transformed MM281 (ST-CorA) strain are from two independent experiments.

(B) Al^{3+} inhibits Mg^{2+} uptake by pFL61-AtMGT10/CM66. Uptake conditions were as described in Figure 2B. Al^{3+} was added at 0 (diamonds), 5 (circles), 10 (triangles), 25 (crosses), and 50 μM (squares).

defect of a Salmonella mutant lacking all three Mg^{2+} transport systems (MM281). Such a mutant strain only survives on media containing 10 mM or higher concentrations of Mg^{2+}, much higher than usually available in Mg^{2+} concentrations in the environment. The mutant strain transformed with *AtMGT1* cDNA grew well even on medium containing as low as 10 μM Mg^{2+} (a 1000-fold increase in Mg^{2+}-acquiring ability), just like the mutant strain containing wild-type CorA protein. These complementation studies in two different systems strongly suggest that AtMGT family proteins mediate Mg^{2+} transport.

Direct evidence for cation uptake was obtained for both genes. Measurement of cellular Mg^{2+} content over a 60-min period demonstrated that the *alr1alr2* yeast mutant transformed with *AtMGT10* cDNA accumulated significantly more Mg^{2+} than did the control strain. For AtMGT1, radioactive Ni^{2+} was used to demonstrate cation uptake conferred by AtMGT1 expression in Salmonella. Kinetic analyses of Ni^{2+} uptake by AtMGT1 expressed in bacteria essentially copied the transport properties of CorA, a proven high-affinity Mg^{2+} transporter in bacteria (Smith and Maguire, 1998). The K_i for Mg^{2+}-mediated inhibition of Ni^{2+} uptake is ~10-fold lower than that for Ni^{2+} itself, suggesting that AtMGT1 and CorA display much higher affinity for Mg^{2+}. The K_m for Ni^{2+} uptake by both AtMGT1 and CorA is in the submillimolar range, significantly higher than the levels of Ni^{2+} encountered by bacteria. These results suggest that AtMGT1, like CorA, does not function as a physiological Ni^{2+} transporter. Furthermore, the cation selectivity studies using the same tracer inhibition assay suggest that AtMGT1 may transport Mg^{2+} with the highest efficiency of all the divalent cations tested. The K_i for Mg^{2+} is under 20 μM for AtMGT1 as compared with submillimolar or millimolar range for other divalent cations, including Fe^{2+}, Mn^{2+}, Cu^{2+}, and Co^{2+} (Figure 7A). The Mg^{2+} concentrations required for tracer inhibition occurs well within the range of Mg^{2+} concentrations found in most soil types (20 to 200 μM; Epstein, 1972) and in plant sap extracts (15 to 60 mM; Baker, 1983). The results of these complementation and uptake assays are entirely consistent with the idea that the AtMGT family of transporters is involved in Mg^{2+} acquisition from the environment and/or in Mg^{2+} transport within the plant. This physiological function has been proposed for all members of the CorA family analyzed to date. However, direct evidence is needed to establish such a role for the AtMGT gene family in planta.

CorA is present as a single member in all bacterial or Archaeal systems (Smith et al., 1998). Mammals also appear to contain a single copy of an *MRS2*-like member of the family. In contrast, the Arabidopsis MGT family contains at least 10 members (Figure 3). Analysis of expressed sequence tags suggests that the family size is large in most plants. Several factors may determine the functional diversity of various family members. The transcript expression pattern of the 10 AtMGT genes suggests that some individual family members may be expressed differently in various tissue and cell types (Figure 4). Aside from the spatial pattern of gene expression, individual AtMGT members may also display different expression patterns during various developmental stages of plants. Furthermore, each member may be localized to the same or different subcellular compartment. Our results suggest that AtMGT1 may be localized to the plasma membrane. There are no obvious chloroplast transit sequences on any of the other family members, although *AtMGT5* and *AtMGT6* contain predicted mitochondrial leaders. Within the *AtMGT* multigene family, there may be both specific and overlapping gene functions performed by the various members, depending on their expression patterns and subcellular localizations. This princi-

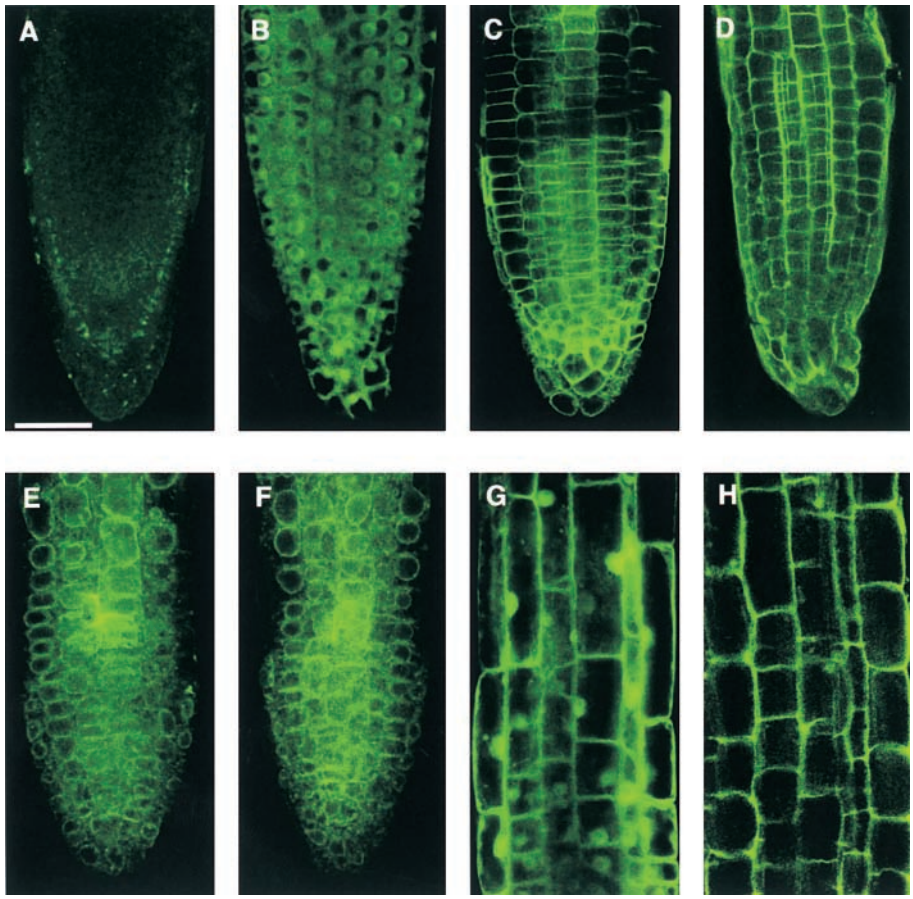

Figure 9. AtMGT1-GFP Fusion Is Localized to the Plasma Membrane.

(A) Background fluorescence of a wild-type Arabidopsis root tip.
(B) Fluorescence from a transformed root tip expressing GFP.
(C) Fluorescence from a transformed root tip expressing cell surface marker fused to GFP (clone 37-26; http://deepgreen.stanford.edu/html/screen/cell%20surface/).
(D) Fluorescence from a transformed root tip expressing AtMGT1-GFP fusion protein.
(E) Same material as in **(C)** after osmolysis.
(F) Same material as in **(D)** after osmolysis.
(G) Fluorescence from a transformed root (elongation zone) expressing GFP.
(H) Fluorescence from a transformed root (elongation zone) expressing AtMGT1-GFP.
Bar in **(A)** = 50 μm for **(A)** to **(H)**.

ple seems to govern other transporter families, especially those responsible for transport of abundant essential elements such as potassium (Maathuis et al., 1997). It is also possible that the different AtMGT family members have different transport properties, because they show significant sequence diversity. For example, AtMGT1 and AtMGT10 share only ~15% amino acid identity. While both appear to transport Mg^{2+}, it remains possible that different AtMGT members have different cation selectivity that contributes to the functional diversity of the protein family.

Although AtMGT1 and AtMGT10 showed transport properties similar to those of the bacterial CorA family, they possess a significant difference in Al^{3+} sensitivity. Our results show that Al^{3+} is a potent inhibitor of both AtMGT1 and AtMGT10 activity. MacDiarmid and Gardner (1996) previously showed that Al^{3+} also inhibits uptake by two yeast members of the CorA family, *ALR1* and *ALR2*, and subsequently showed that overexpression of either gene conferred aluminum tolerance on yeast (MacDiarmid and Gardner, 1998). Al^{3+} toxicity in higher plants is a significant agricultural problem, but the mechanism of toxicity remains a matter of debate (Kochian, 1995). There is some evidence

that Mg^{2+} transport may be important, however. First, Mg^{2+} deficiency is induced in Al-treated grasses and cereals (Tan et al., 1991), and application of higher levels of Mg^{2+} can reduce Al toxicity (Tan et al., 1991; Matsumoto, 2000). Second, direct uptake experiments have shown that Al inhibits Mg^{2+} uptake by roots (Rengel and Robinson, 1989). Our study provides a possible molecular target for Al^{3+} inhibition of Mg^{2+} uptake in plants. Because AtMGT1 and AtMGT10 activity was inhibited by relatively low concentrations of Al^{3+}, we propose that the AtMGT transport system is inhibited by Al^{3+}, leading to Al-induced Mg^{2+} deficiency in higher plants. Further molecular genetic experiments will determine whether AtMGT members can be genetically engineered to improve Al tolerance in plants.

METHODS

Yeast Strains and Culture Conditions

The isogenic *Saccharomyces cerevisiae* strains CM66 (MATa *alr1*::*HIS3 alr2*::*TRP1 his3-Δ200, ura3-52, leu2-Δ1,* and *lys2-Δ202 trp1-Δ63*) and CM52 (MATa *his3-Δ200, ura3-52, leu2-Δ1,* and *lys2-Δ202 trp1-Δ63*) derived from FY833 (Winston et al., 1995), and both were obtained from segregation of a single tetrad (C.W. MacDiarmid, unpublished data). CM66 was generated by sequential one-step gene disruption (Kaiser et al., 1994) using an *alr1*::*HIS3* polymerase chain reaction (PCR) product (MacDiarmid and Gardner, 1998) and a *palr2*::*TRP1* plasmid (analogous to pALR:URA3; see MacDiarmid and Gardner, 1998). Yeast strains were grown on standard synthetic media (SD) or complete media (YPD), as described by Sherman (1991), with the appropriate auxotrophic supplements and 2% glucose. Media were supplemented with 250 mM $MgCl_2$ (referred to as SDM and YPDM) as indicated. For growth on Mg^{2+} concentrations of <4 mM, LPM minimal media was used (MacDiarmid and Gardner, 1996). pFLN2 was derived from the pFL61 high copy number plasmid (Minet et al., 1992) by the addition of XhoI and SalI sites to the multiple cloning region (C.W. MacDiarmid, unpublished data). pFLN2 was used to express *ALR1* from the constitutive yeast phosphoglycerate kinase promoter.

Screening of Arabidopsis Library in Yeast

An Arabidopsis cDNA library cloned into yeast expression vector pFL61 (Minet et al., 1992) was used to transform the yeast mutant strain CM66 using the method of Gietz et al. (1995). Total transformants were estimated by plating on medium lacking uracil but containing high Mg^{2+} (SDM-ura). In parallel, putative Mg^{2+} transport genes were obtained by selecting for the ability to grow on 4 mM Mg^{2+} (SD-ura plates). Yeast plasmids were rescued in *Escherichia coli* and retransformed into CM66 to confirm that their ability to confer growth on normal levels of Mg^{2+} was encoded by the plasmid.

Measurement of Mg^{2+} by Atomic Absorption Spectroscopy

All glass- and plasticware were soaked with concentrated HNO_3 overnight and washed extensively with milli-Q water (Millipore Corporation, Molsheim, France). Yeast strains were grown to log phase ($OD_{600} = 0.6$ to 0.8) in LPM medium containing 250 mM $MgCl_2$. The cell cultures were washed twice with milli-Q water and incubated at the same density in LPM media without $MgCl_2$ for 24 hr. After incubation, the cultures were centrifuged at 500*g* for 2 min, resuspended in 5 mM Tris-succinate buffer, pH 4, supplemented with 1% glucose and incubated for 30 min at 25°C. The yeast cultures were centrifuged at 500*g*, and the pellet was resuspended in 5 mM Tris-succinate buffer, pH 4, supplemented with 4 mM $MgCl_2$. Samples of 10 mL were drawn at indicated time points, washed three times in 10 mL of the following solutions (milli-Q water, 1 mM EDTA, milli-Q water), and then resuspended in 2 mL of milli-Q water. A 0.5-mL sample was taken to measure the final OD_{600}, and the remaining 1.5 mL was mixed with an equal volume of concentrated HNO_3, incubated at 100°C for 1 hr, and diluted with 2 volumes of $LaCl_2$ buffer (240 mM HCl and 10 mM $LaCl_2$). The Mg content was measured in a Varian 1275 atomic absorption spectrophotometer (Palo Alto, CA) using an air-acetylene flame at a wavelength of 285.2 nm.

Reverse Transcription–PCR Amplification of *AtMGT* Genes

Total RNA (Figure 3, lanes 2 to7, provided by S. Fowler) was prepared as described by Whitelam et al. (1993), but omitting the final LiCl precipitation step. RNA for lanes 8 and 9 (provided by K. Richards) was prepared as described by Richards et al. (1998). The RNA samples were treated with 468.6 international units (IU) of DNase in the presence of 40 IU of RNase inhibitor, RNaseOUT (Gibco BRL, Rockville, MD), then passed through an RNA cleanup kit (RNA-EASY; Qiagen, Germantown, MD), eluted in 50 μL of water, dried down, and resuspended in 9.5 μL of water. An aliquot of 0.5 μL of reverse transcription (RT) adapter primer g775 $(dT)_{17}$ (Frohman et al., 1988) was added; the mix was incubated for 10 min at 70°C and then placed on ice for 5 min. The final reaction mix for the first-strand synthesis contained 50 mM Tris-HCl, pH 8.3, 75 mM KCl, 3 mM $MgCl_2$, 10 mM DTT, and 2 mM each dNTP, and was incubated at 42°C for 2 hr. The completed reaction was diluted to 200 μL and was stored at −20°C before amplification.

The primers used in PCR amplification of the *AtMGT* genes are as follows: AtMGT1, 5′-CTCGAGGTCGACTGGTTTTGTAGTATCTGGAG-3′ and 5′-CCGCCGCGTGTCAGGGTAGTTATGTC; AtMGT2, 5′-CTCGAGGTCGACTATTTGGCATTTCAGTATCT-3′ and 5′-CCGCCGAAGATTCCATTGTGTAAAGG-3′; AtMGT3, 5′-GTCGACAAACATGGGAGAACAACTAGATCCA-3′ and 5′-GCGGCCGCCTAAGCTCAGCAAAAGACATTAG-3′; AtMGT4, 5′-CTCGAGGTGAAGGAGACGGATAAAAA-3′ and 5′-CCGCCGCACTTCCAACATTCCTCAGC-3′; AtMGT5, 5′-CTCGAGGTCGACAAACATGGGATCACTTCGCCGTA-3′ and 5′-CCGCGGCCACAAAGCTAATCTCATAATGACT-3′; AtMGT6, 5′-GTCGACAAACGATCTCTGACCTGCGACGAAGAAGTTGACTGAA-3′ and 5′-CCGCGGTATATCATTTCCATCTACATGTGTTCCTCAACAA-3′; AtMGT7, 5′-CTCGAGGTCGACAAAGATGTCACCTGACGGAGAACT and 5′-CCGCGGAATGCTGGCGAGAAGAGACC; AtMGT8, 5′-CTCGAGGTCGACAAAGATGTTGCCTAACGAAGAAC-3′ and 5′-CCGCGGCCTTCCATCGTCAAAAACCA-3′; AtMGT9, 5′-GTCGACAAACCATGGCGCAAAACGGGT-3′ and 5′-CCGCGGTGCCCCTTCACAATCTCTCC-3′; and AtMGT10, 5′-CCTTCCTTTTCTCTCCAG-3′ and 5′-AATCCACCCGTTGTTA-3′.

For *AtMGT1*, *AtMGT4*, *AtMGT8*, and *AtMGT10*, a touchdown PCR cycle was used, with an initial hold at 96°C for 2 min; 40 cycles each consisting of a 30-sec denaturing step at 96°C, an annealing step (initially at 65°C, decreasing by 0.5°C per cycle over the next 19 cy-

cles, followed by a further 20 cycles at 55°C annealing), 72°C elongation for 60 sec; and a final extension of 8 min at 72°C. PCR cycles for the other six genes consisted of the following: an initial heating at 96°C for 2 min; 35 (*AtMGT6*) or 30 (remainder) cycles of 96°C denaturation for 30 sec, 58°C annealing for 30 sec, and 72°C elongation for 30 sec; and a final extension of 8 min at 72°C. PCR was in 2 mM $MgCl_2$, 20 mM Tris-HCl, pH 8.4, 50 mM KCl, 0.2 mM of each dNTP, with 1 U of platinum Taq (Gibco BRL).

Amplification and Sequencing of AtMGT cDNAs

Using the primers listed above, cDNAs corresponding to *AtMGT1* to *AtMGT4* and *AtMGT6* to *AtMGT9* were amplified from the Lacroute library (Minet et al., 1992); flower cDNA was used for *AtMGT5*. The single-stranded sequences of one to three clones of each cDNA were then compared with the genomic copies to identify intron locations (see below). Most cDNAs contained from zero to seven nucleotide differences from the genomic copy, consistent with PCR errors, sequencing errors, and/or real nucleotide differences between ecotypes (the genome sequence is from ecotype Columbia; the cDNA copies were all Landsberg). However, *AtMGT7* had 18 nucleotide differences that resulted in six amino acid substitutions between the genomic and amplified cDNA copy; all of these differences were conserved in two copies sequenced.

For each *AtMGT* gene, the GenBank accession number of the corresponding genomic sequence is listed below, along with the predicted protein sequence encoded by the genomic copy; for five genes, intron locations obtained from the cDNA sequence differed from those predicted: *AtMGT1*, AC011713, aff14678; *AtMGT*, AC010924, aff18497; *AtMGT3*, AC006836, add20070; *AtMGT4*, AP000417, bab02549; *AtMGT5*, AL161573, similar to cab81446 but with the location of the first intron changed; *AtMGT6*, AL163527, similar to cab86925 but with the first intron missing, so that a different reading frame with a different start codon is used at the N terminus; *AtMGT7*, AL353994, similar to cab89361 but with two changed internal splice sites; *AtMGT8*, AL353994, similar to cab89358 but with three changed internal splice sites; *AtMGT9*, AB010076, bab11423; and *AtMGT10*, AB005243, similar to bab10604 but with an extra 3′ intron added that alters the reading frame at the C terminus.

Salmonella typhimurium Mutant Complementation

The *S. typhimurium* mutant MM281, which lacks *CorA*, *MgtA*, and *MgtB* genes, and MM1927 (MM281 transformed with CorA gene) were gifts from Dr. M. Maguire (Townsend et al., 1995). For the complementation experiment, MGT1 cDNA was inserted into a λYES *E. coli*/yeast shuttle vector that was provided by Dr. R. Davis (Elledge et al., 1991). MM281 cells were transformed with λYES vector and λYES-MGT1 plasmid by electroporation. Cells were plated onto Luria-Bertani (LB) medium supplemented with 100 mM Mg^{2+} and appropriate antibiotics (50 μg/mL ampicillin, 34 μg/mL chloramphenicol, and 50 μg/mL kanamycin), and incubated at 37°C overnight. The transformants were confirmed by PCR amplification of both the vector and MGT1 coding sequence. Individual transformants were grown in Lennox Base (LB) liquid medium containing the same concentrations of Mg^{2+} and antibiotics. MM1927 containing Salmonella *CorA* gene was used as a positive control. The cultures were adjusted to 1.0 OD_{600}, diluted in a 10-fold series, and spotted (2 μL) onto N-minimal medium supplemented with different concentrations of $MgSO_4$ and the antibiotics. Growth of different strains was scored after incubation at 37°C for 2 days.

Tracer Uptake Assays

Uptake of ^{63}Ni was performed as described previously (Snavely et al., 1989; Smith et al., 1998). ^{63}Ni uptake was assayed using strain MM1927 (MM281-STCorA) for *S. tyhiumurium* CorA and MM281-MGT1 for MGT1. MM281 was used as a negative control. Briefly, bacterial cultures of different strains were grown overnight in LB broth containing 100 mM Mg^{2+} and the appropriate antibiotics. Cells were washed with N-minimal medium without added Mg^{2+} and then diluted 1:5 in N-minimal medium containing 1 mM Mg^{2+} and appropriate antibotics. After a 3-hr subculture, cells were collected by centrifugation at 1000*g* for 15 min and washed twice with ice-cold Mg^{2+}-free N-minimal medium. The washed cells were resuspended in the same medium and adjusted to 1.0 OD_{600}. For a standard assay, uptake was initiated by adding 0.2 mL of cells to 0.8 mL of N-minimal medium containing 100 μM $NiCl_2$ and 0.5 μCi of $^{63}Ni^{2+}$. For the inhibition assay of tracer uptake, various concentrations of divalent cations were included in the assay buffer. Typically, uptake was stopped at 5 min by adding 1 mL of ice-cold washing buffer. Cells were washed four times with 1.5 mL of ice-cold washing buffer, and $^{63}Ni^{2+}$ activity associated with cells was determined by a scintillation counter (model LS600IC; Beckman Instruments). The relative tracer uptake was standardized against the maximal value and presented as a percentage of maximal uptake.

Subcellular Localization of MGT1-GFP Fusion Protein

The AtMGT1 coding region was fused to green fluorescent protein (GFP) coding region in binary vector pMD1 that contains the cauliflower mosaic virus 35S promoter followed by a short polylinker, GFP coding region, and the nopaline synthase terminator region (Sheen et al., 1995). The AtMGT1 cDNA without a stop codon was inserted into the polylinker region to form an in-frame fusion with the GFP coding region. This construct was used to transform wild-type Arabidopsis plants (Columbia ecotype) by vacuum infiltration. Transformants were selected on 0.5 × Murashige and Skoog medium supplemented with 1% [w/v] sucrose, 0.8% [w/v] agar, and 50 μg/mL kanamycin) and were propagated in the soil. T2 seedlings were used to localize GFP fluorescence by a confocal microscope (model 510 UV/Vis; Zeiss, Heidelberg, Germany). The images were processed by Adobe Photoshop (San Jose, CA).

ACKNOWLEDGMENTS

We thank Dr. Michael E. Maguire for providing bacterial strains and advice on tracer uptake assays. We are indebted to Drs. David Ehrhardt and Yong-Hwa Cheong for transgenic plants expressing cell surface marker fused to GFP and GFP alone, respectively. We also thank Sarah Fowler and Keith Richards for providing RNA samples; Colin MacDiarmid for constructing strain CM66 and the vector pFLN2; Glenn Boyes for AAS measurements; and Jo Putterill, Colin

MacDiarmid, Keith Richards, Trent Bosma, and Jeannette Keeling for critical reading of the manuscript. A.F.T. was the recipient of a Queen Elizabeth II Auckland City Council Award; R.S.M.D. was the recipient of an AGMARDT Postgraduate Fellowship. This project is funded by a grant from the New Zealand Foundation for Research Science and Technology (R.C.G.) and by a USDA-NRI grant (S.L.).

Received August 14, 2001; accepted September 4, 2001.

REFERENCES

Baker, D.A. (1983). Uptake of cations and their transport within the plant. In Metals and Micronutrients: Uptake and Utilisation, D.A. Robb and W.S. Pierpoint, eds (London: Academic Press), pp 3–19.

Blanc, G., Barakat, A., Guyot, R., Cooke, R., and Delseny, M. (2000). Extensive duplication and reshuffling in the Arabidopsis genome. Plant Cell **12,** 1093–1102.

Bui, D.M., Gregan, J., Jarosch, E., Ragnini, A., and Schweyen, R.J. (1999). The bacterial magnesium transporter CorA can functionally substitute for its putative homologue Mrs2p in the yeast inner mitochondrial membrane. J. Biol. Chem. **274,** 20438–20443.

Elledge, S.J., Mulligan, J.T., Ramer, S.W., Spottswood, M., and Davis, R.W. (1991). Lambda YES: A multifunctional cDNA expression vector for the isolation of genes by complementation of yeast and *Escherichia coli* mutations. Proc. Natl. Acad. Sci. USA **88,** 1731–1735.

Epstein, E. (1972). Mineral Nutrition of Plants: Principles and Perspectives. (New York: John Wiley).

Frohman, M.A., Dush, M.K., and Martin, G.R. (1988). Rapid production of full-length cDNAs from rare transcripts: Amplification using a single gene-specific oligonucleotide primer. Proc. Natl. Acad. Sci. USA **85,** 8998–9002.

Gibson, M.M., Bagga, D.A., Miller, C.G., and Maguire, M.E. (1991). Magnesium transport in *Salmonella typhimurium*: The influence of new mutation conferring Co^{2+} resistance on the CorA Mg^{2+} transporter system. Mol. Microbiol. **5,** 2753–2762.

Gietz, D., Schiestl, R.H., Willems, A.R., and Woods, R.A. (1995). Studies on the transformation of intact yeast cells by the LiAc/SS–DNA/PEG Procedure. Yeast **11,** 355–360.

Joslin, J.D., Kelly, J.M., Wolfe, M.H., and Rustad, L.E. (1988). Elemental patterns in roots and foliage of mature spruce across a gradient of soil aluminum. Water Air Soil Pollut. **40,** 375–390.

Kaiser, C., Michaelis, S., and Mitchell, A. (1994). Methods in Yeast Genetics: A Cold Spring Harbor Laboratory Course Manual. (Cold Spring Harbor, NY: Cold Spring Harbor Laboratory Press).

Kochian, L.V. (1995). Cellular mechanisms of aluminum toxicity and resistance in plants. Annu. Rev. Plant Physiol. Plant Mol. Biol. **46,** 237–260.

Kucharski, L.M., Lubbe, W.J., and Maguire, M.E. (2000). Cation hexaammines are selective and potent inhibitors of the CorA Magnesium transporter system. J. Biol. Chem. **275,** 16767–16773.

Maathuis, F.J., Ichida, A.M., Sanders, D., and Schroeder, J.I. (1997). Roles of higher plant K^+ channels. Plant Physiol. **114,** 1141–1149.

MacDiarmid, C.W., and Gardner, R.C. (1996). Al toxicity in yeast: A role for magnesium? Plant Physiol. **112,** 1101–1109.

MacDiarmid, C.W., and Gardner, R.C. (1998). Overexpression of the *Saccharomyces cerevisiae* magnesium transport system confers resistance to aluminum ion. J. Biol. Chem. **273,** 1727–1732.

Maguire, M.E. (1992). MgtA and MgtB: Prokaryotic P-type ATPases that mediate Mg^{2+} influx. J. Bioenerg. Biomembr. **24,** 319–328.

Matsumoto, H. (2000). Cell biology of aluminum toxicity and tolerance in higher plants. Int. Rev. Cytol. **200,** 1–46.

Minet, M., Dufour, M.E., and Lacroute, M. (1992). Complementation of *Saccharomyces cerevisiae* auxotrophic mutants by *Arabidopsis thaliana* cDNAs. Plant J. **2,** 417–422.

Moncrief, M.B., and Maguire, M.E. (1999). Magnesium transport in prokaryotes. J. Biol. Inorg. Chem. **4,** 523–527.

Rees, D.C., Chang, G., and Spencer, R.H. (2000). Crystallographic analyses of ion channels: Lessons and challenges. J. Biol. Chem. **275,** 713–716.

Rengel, Z., and Robinson, D.L. (1989). Competitive aluminum ion inhibition of net magnesium ion uptake by intact *Lolium multiflorum* roots. Plant Physiol. **91,** 1407–1413.

Richards, K.D., Schott, E.J., Sharma, Y.K., Davis, K.R., and Gardner, R.C. (1998). Aluminium induces oxidative stress genes in *Arabidopsis*. Plant Physiol. **116,** 409–418.

Shaul, O., Hilgemann, D.W., de-Almeida-Engler, J., Van Montagu, M., Inze, D., and Galili, G. (1999). Cloning and characterization of a novel Mg^{2+}/H^+ exchanger. EMBO J. **18,** 3973–3980.

Sheen, J., Hwang, S., Niwa, Y., Kobayashi, H., and Galbraith, D.W. (1995). Green-fluorescent protein as a new vital marker in plant cells. Plant J. **8,** 777–784.

Sherman, F. (1991). Getting started with yeast. Methods Enzymol. **194,** 3–20.

Smith, R.L., and Maguire, M.E. (1998). Microbial magnesium transport: Unusual transporters searching for identity. Mol. Microbiol. **28,** 217–226.

Smith, R.L., Banks, J.L., Snavely, M.D., and Maguire, M.E. (1993). Sequence and topology of the CorA magnesium transport systems *of Salmonella typhimurium* and *Escherichia coli*. Identification of a new class of transport protein. J. Biol. Chem. **268,** 14071–14080.

Smith, R.L., Gottlieb, E., Kucharski, L.M., and Maguire, M.E. (1998). Functional similarity between archaeal and bacterial CorA magnesium transporters. J. Bacteriol. **180,** 2788–2791.

Snavely, M.D., Florer, J.B., Miller, C.G., and Maguire, M.E. (1989). Magnesium transport in *Salmonella typhimurium*: $^{28}Mg^{2+}$ transport by the CorA, MgtA, and MgtB systems. J. Bacteriol. **171,** 4761–4766.

Snavely, M.D., Gravina, S.A., Cheung, T.T., Miller, C.G., and Maguire, M.E. (1991). Magnesium transport in *Salmonella typhimurium*. Regulation of mgtA and mgtB expression. J. Biol. Chem. **266,** 824–829.

Szegedy, M.A., and Maguire, M.E. (1999). The CorA Mg^{2+} transport protein of *Salmonella typhimurium*. Mutagenesis of conserved residues in the second membrane domain. J. Biol. Chem. **274,** 36973–36979.

Tan, K., Keltjens, W.G., and Findenegg, G.R. (1991). Role of magnesium in combination with liming in alleviating acid-soil stress

with the aluminum-sensitive sorghum genotype CV323. Plant Soil **136,** 65–72.

Townsend, D.E., Esenwine, A.J., George, J.R., Bross, D., Maguire, M.E., and Smith, R.L. (1995). Cloning of the mgtE Mg^{2+} transporter from *Providencia stuartii* and the distribution of mgtE in the eubacteria. J. Bacteriol. **177,** 5350–5354.

Whitelam, G.C., Johnson, E., Peng, J., Carol, P., Anderson, M.L., Cowl, J.S., and Harberd, N.P. (1993). Phytochrome A null mutants of *Arabidopsis* display a wild-type phenotype in white light. Plant Cell **5,** 119–125.

Winston, F., Dollard, C., and Ricupero-Hovasse, S.L. (1995). Construction of a set of convenient *Saccharomyces Cerevisiae* strains that are isogenic to S288C. Yeast **11,** 53–55.

Zsurka, G., Gregan, J., and Schweyen, R.J. (2001). The human mitochondrial Mrs2 protein functionally substitutes for its yeast homologue, a candidate magnesium transporter. Genomics **72,** 158–168.

NOTE ADDED IN PROOF

While earlier versions of this manuscript were in review, a related paper (**Schock, I., Gregan, J., Steinhauser, S., Schweyen, R., Brennicke, A., and Knoop, V.** [2000]. A member of a novel *Arabidopsis thaliana* gene family of candidate Mg^{2+} ion transporters complements a yeast mitochondrial group II intron-splicing mutant. Plant J. **24,** 489–501) appeared showing that the gene referred to here as *AtMGT2* complements a yeast *Mrs2* mutant.